Two–Way Communications via Reconfigurable Intelligent Surface

Saman Atapattu*, Rongfei Fan†, Prathapasinghe Dharmawansa‡, Gongpu Wang§ and Jamie Evans*
*Department of Electrical and Electronic Engineering, University of Melbourne, Victoria, Australia
†School of Information and Electronics, Beijing Institute of Technology, Beijing 100081, P. R. China
‡Department of Electronic and Telecomm. Engineering, University of Moratuwa, Moratuwa, Sri Lanka
§School of Computer and Information Technology, Beijing Jiaotong University, Beijing 100044, P. R. China
Email:*{saman.atapattu, jse}@unimelb.edu.au; †fanrongfei@bit.edu.cn; ‡prathapa@uom.lk; §gpwang@bjtu.edu.cn

***Abstract*—The novel reconfigurable intelligent surface (RIS) is an emerging technology which facilitates high spectrum and energy efficiencies in Beyond 5G and 6G wireless communication applications. Against this backdrop, this paper investigates two–way communications via reconfigurable intelligent surfaces (RISs) where two users communicate through a common RIS. We assume that uplink and downlink communication channels between two users and the RIS can be reciprocal. We first obtain the optimal phase adjustment at the RIS. We then derive the exact outage probability and the average throughput in closed-forms for single-element RIS. To evaluate multiple-element RIS, we first introduce a gamma approximation to model a product of Rayleigh random variables, and then derive approximations for the outage probability and the average throughput. For large average signal-to-interference-plus-noise ratio (SINR) ρ, asymptotic analysis also shows that the outage decreases at the rate $(\log(\rho)/\rho)^L$ where L is the number of elements, whereas the throughput increases with the rate $\log(\rho)$.**

***Index Terms*—Outage probability, reconfigurable intelligent surface (RIS), throughput, two–way communications.**

I. Introduction

Radio signal propagation via man-made intelligent surfaces has emerged recently as an attractive and smart solution to replace power-hungry active components [1]. This is a newly proposed concept beyond multi-input multi-output (MIMO) or massive MIMO systems and relaying networks [2]–[4]. This novel concept utilizes electromagnetically controllable surfaces that can be integrated into the existing infrastructure. Such a surface is frequently referred to as Reconfigurable Intelligent Surface (RIS), Large Intelligent Surface (LIS) or Intelligent Reflective Surface (IRS). While a relay actively processes the received signal before re-transmitting the signal, the RIS passively reflects the signal without processing. Since the RIS-assisted communication outperforms the conventional relaying techniques in terms of energy efficiency [5], the RIS can address several major issues arising from Beyond 5G and 6G wireless applications. This brand-new concept has already been proposed to incorporated into various wireless techniques, and most existing work on RIS focus on phase optimization of RIS elements [5]–[8]. However, there are very limited research efforts explored the communication-theoretic performance limits [9]–[12].

This work is supported in part by the Australian Research Council (ARC) through the Discovery Early Career Researcher (DECRA) Award under Grant DE160100020 and in part by the Discovery Project (DP) under Grant DP180101205.

A. Related Work

An IRS-enhanced point-to-point multiple-input single-output (MISO) system was considered in [6], which aimed to maximize the total received signal power at the user. For downlink multi-user communication, both the transmit power allocation and the phase shifts of the reflecting elements were designed to maximize the energy efficiency in [5]. Moreover, physical layer security issues were considered in [7], [8].

A very few more recent work have focused on analytical performance evaluation. For an LIS-assisted large-scale antenna system, an upper bound on the ergodic capacity was first derived and then a procedure for phase shift design based on the upper bound was discussed in [9]. An asymptotic analysis of the uplink data rate and the channel hardening effect in a large antenna-array system were presented in [10]. For a large RIS system, some theoretical performance limits were also explored in [11] using the central limit theorem (CLT). The LIS transmission with phase errors was considered in [12].

On the other hand, two–way communications exchange messages of two or more users over the same shared channel [13]. Since this improves the spectral efficiency of wireless system such as massive MIMO, full-duplex communications, NOMA, mmWave communications, and cognitive radio, the RIS may also serve as a potential candidate for further performance improvement in the two–way Beyond 5G or 6G systems. However, to the best of our knowledge, all these previous work on RIS considered the one–way communications. Motivated by this reason, as the first work, we study the RIS for two–way communications in view of quantifying the performance limits, which is the novelty of this paper.

B. Summary of Contributions

The main contributions of the paper are summarized as follows:

1) *For a single-element RIS*, we first derive the exact outage probability and throughput in closed-forms for the optimal phase adjustment at the RIS. We then provide asymptotic results for sufficiently large transmit power

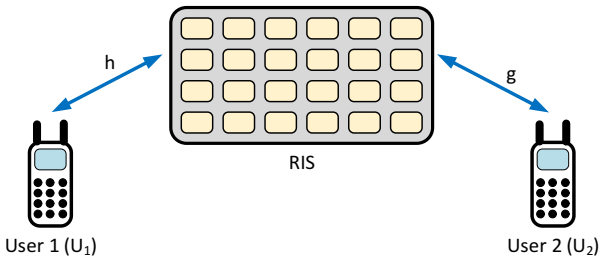

Fig. 1: Two–way communications via RIS.

compared to the noise and interference powers. Our analysis reveals novel observations.

2) *For a multiple-element RIS*, where the number of elements, L, is more than one but not necessary as large as in LIS. In this respect, the instantaneous SINR turns out to take the form of a sum of product of two Rayleigh random variables (rvs). As well documented in the literature, this does not admit a tractable PDF or CDF expression. To circumvent this problem, we first approximate the product of two Rayleigh rvs with a Gamma rv, and then evaluate the outage probability and throughput. This seems to be the first paper which uses gamma approximation for a Rayleigh product. Surprisingly, this approximation works well and more accurate than the CLT approximation (which was frequently used in LIS).

II. System Model

A reconfigurable intelligent surface (RIS) aided two–way wireless network has two end users (namely, U_1 and U_2) and a reflective surface (R), as depicted in Fig. 1. The two users exchange their information symbols concurrently via the RIS. Each user is equipped with a pair of antennas for the transmission and reception. The RIS, which consists of passive components, only adjusts the phases of incident signals. The RIS contains L reconfigurable reflectors where the ℓth passive element is denoted as I_ℓ. No direct link between two users is assumed, due to transmit power limitation or the severe shadowing effect. The unit-energy information symbols from U_1 and U_2, randomly selected from the codebook, are denoted by s_1 and s_2, respectively. The power budgets are P_1 and P_2 for end users U_1 and U_2, respectively. We assume all fading channels are independent (placing the antennas of users and elements of RIS sufficiently apart) and reciprocal (overall uplink and downlink transmission time falls within a coherence interval of the channel).

We denote the fading coefficients from U_1 to the I_ℓ and from U_2 to the I_ℓ as $h_\ell = \alpha_\ell \mathrm{e}^{-j\varphi_\ell}$ and $g_\ell = \beta_\ell \mathrm{e}^{-j\psi_\ell}$, respectively. The channels are reciprocal such that the channel gains from the I_ℓ to the two end users are also h_ℓ and g_ℓ, respectively. All channels are assumed to be independent and identically distributed (i.i.d.) complex Gaussian fading with zero-mean and σ^2 variance, i.e., $h_\ell, g_\ell \sim \mathcal{CN}(0, \sigma^2)$. Therefore, magnitudes of h_ℓ and g_ℓ (i.e., α_ℓ and β_ℓ) follow Rayleigh distributions. It is assumed that the two end users know all channel coefficients, $h_1, \ldots, h_L$ and $g_1, \ldots, g_L$, and the I_ℓ knows its own channels' phase values φ_ℓ and ψ_ℓ.

Each user receives a superposition of the two signals via the RIS. Thus, the receive signal at U_1 at time t can be given as

$$y_1(t) = \underbrace{\sqrt{P_2}\left(\sum_{\ell=1}^{L} g_\ell \mathrm{e}^{j\phi_\ell} h_\ell\right) s_2(t)}_{\text{Desired signal}} + \underbrace{i_1(t)}_{\text{Loop interference}} + \underbrace{\sqrt{P_1}\left(\sum_{\ell=1}^{L} h_\ell \mathrm{e}^{j\phi_\ell} h_\ell\right) s_1(t)}_{\text{Self interference}} + \underbrace{w_1(t)}_{\text{Noise}} \quad (1)$$

where ϕ_ℓ is the adjustable phase induced by the I_ℓ, $i_1(\tau)$ is the receive residual self-interference resulting from several stages of cancellation and $w_1(t)$ is the additive white Gaussian noise (AWGN) at U_1 which is assumed to be i.i.d. with the distribution $\mathcal{CN}(0, \sigma_{w_1}^2)$. Since the U_1 has the global CSI, it can completely eliminate the self-interference. To avoid loop interference, similar to full-duplex communications, the U_1 applies some sophisticated loop interference cancellations, which results in residual interference [14]. Among different models used in the literature of full-duplex communications, in this paper, we adopt the model where $i_1(t)$ is i.i.d. with zero-mean, $\sigma_{i_1}^2$ variance, additive and Gaussian. Further, the variance is modeled as $\sigma_{i_1}^2 = \omega P_1^\nu$ for $P_1 \geq 1$, where the two constants, $\omega > 0$ and $\nu \in [0, 1]$, depend on the cancellation scheme used at the user. Thus, the instantaneous SINR at user k, U_k, $k \in \{1, 2\}$ is given as

$$\gamma_k = \rho_k \left| \sum_{\ell=1}^{L} \alpha_\ell \beta_\ell \mathrm{e}^{j(\phi_\ell - \varphi_\ell - \psi_\ell)} \right|^2, \quad (2)$$

where $\rho_1 = \frac{P_2}{\sigma_{i_1}^2 + \sigma_{w_1}^2}$ and $\rho_2 = \frac{P_1}{\sigma_{i_2}^2 + \sigma_{w_2}^2}$ are the average SINR.

III. Performance Analysis

A. Optimum Phase Design at RIS

A careful inspection of the structures of γ_k reveals that the optimal ϕ_ℓ, which maximizes the instantaneous SINR of each user, admits the form

$$\phi_\ell^\star = \varphi_\ell + \psi_\ell \quad \text{for } \ell = 1, \cdots, L. \quad (3)$$

This is usually feasible at the RIS as it has the global phase information of the respective channels. Now, the maximum SINRs at U_k can be given as

$$\gamma_k^\star = \rho_k \left(\sum_{\ell=1}^{L} \alpha_\ell \beta_\ell \right)^2 = \rho \left(\sum_{\ell=1}^{L} \zeta_\ell \right)^2 ; \ \zeta_\ell = \alpha_\ell \beta_\ell, \quad (4)$$

where, without loss of generality, we assume $P_1 = P_2 = P$, $\sigma_{i_1}^2 = \sigma_{i_2}^2 = \sigma_i^2$ and $\sigma_{w_1}^2 = \sigma_{w_2}^2 = \sigma_w^2$, and we thus have $\rho = \frac{P}{\sigma_i^2 + \sigma_w^2}$

B. Outage Probability

By definition, the outage probability of each user can be expressed as $P_{\text{out}} = \mathsf{Pr}[\gamma \le \gamma_{\text{th}}]$, where γ_{th} is the SINR threshold. This in turn gives us the important relation

$$P_{\text{out}} = F_{\gamma}(\gamma_{\text{th}}), \tag{5}$$

where $F_{\gamma}(x)$ is the cumulative distribution function (CDF) of γ.

1) When $L = 1$: In this case, the instantaneous SINR of each user is $\gamma = \rho\zeta_1^2 = \rho(\alpha_1\beta_1)^2$. Since α_1 and β_1 are identical Rayleigh rvs with parameter σ, the PDF and CDF expressions can be written as $f_X(x) = (2x/\sigma^2)\,\mathrm{e}^{-x^2/\sigma^2}$ and $F_X(x) = 1 - \mathrm{e}^{-x^2/\sigma^2}$, respectively. The outage probability can be derived as

$$\begin{aligned} P_{\text{out}|\text{L}=1}(\gamma_{\text{th}}) &= \int_0^{\infty} F_{\alpha_1}\left(\sqrt{\frac{\gamma_{\text{th}}}{\rho}}\frac{1}{x}\right) f_{\beta_1}(x)\,\mathrm{d}x \\ &= 1 - \frac{2}{\sigma^2}\sqrt{\frac{\gamma_{\text{th}}}{\rho}}\mathsf{K}_1\left(\frac{2}{\sigma^2}\sqrt{\frac{\gamma_{\text{th}}}{\rho}}\right) \end{aligned} \tag{6}$$

where the last equality results from $\int_0^{\infty}\mathrm{e}^{-\frac{b}{4x}-ax}\mathrm{d}x = \sqrt{\frac{b}{a}}\mathsf{K}_1\left(\sqrt{ab}\right)$ with $\mathsf{K}_n(\cdot)$ denoting the modified Bessel function of the second kind [15, eq. 3.324.1].

2) When $L \ge 2$: For this case, let us now focus on deriving the CDF of the rv $\zeta = \sum_{\ell=1}^{L}\zeta_\ell$ where the exact CDF of ζ_ℓ is

$$F_{\zeta_\ell}(t) = 1 - \frac{2t}{\sigma^2}\mathsf{K}_1\left(\frac{2t}{\sigma^2}\right) \tag{7}$$

However, by using the exact CDF, an exact statistical characterization of the CDF ζ seems an arduous task. To circumvent this difficulty, in what follows we first seek an approximation for the PDF and CDF of ζ_ℓ. Among different techniques of approximating distributions [16], the following lemma gives the Gamma approximation for the CDF $F_{\zeta_1}(t)$.

Lemma 1: The distribution of the product of two i.i.d. Rayleigh rvs with parameter σ can be approximated with a Gamma distribution which has the CDF

$$F_{\zeta_\ell}(t) \approx \frac{1}{\Gamma(k)}\gamma\left(k, \frac{t}{\theta}\right) \tag{8}$$

where $k = \frac{\pi^2}{(16-\pi^2)}$ and $\theta = \frac{(16-\pi^2)\sigma^2}{4\pi}$ and $\gamma(\cdot,\cdot)$ is the lower incomplete gamma function [15].

Proof: Since the first and second moments of ζ_ℓ in (7) are $\mathsf{E}[\zeta_\ell] = \pi\sigma^2/4$ and $\mathsf{E}\left[\zeta_\ell^2\right] = \sigma^4$, the rv ζ_ℓ has $\pi\sigma^2/4$ mean and $(16-\pi^2)\sigma^4/16$ variance. By matching the mean and variance of the rv ζ_ℓ with the $k\theta$ mean and $k\theta^2$ variance of the regular Gamma distribution, we have the above CDF. ∎

Now we compare the accuracy of the approximation with that of the exact. One of the possible measures of accuracy is the Kullback-Leibler (KL) divergence ($\mathcal{D}_{\text{KL}}$) which is defined as [16]

$$\mathcal{D}_{\text{KL}}(\sigma) = \int_{-\infty}^{\infty} f_{\text{Ext}}(x)\log\frac{f_{\text{Ext}}(x)}{f_{\text{App}}(x)}dx.$$

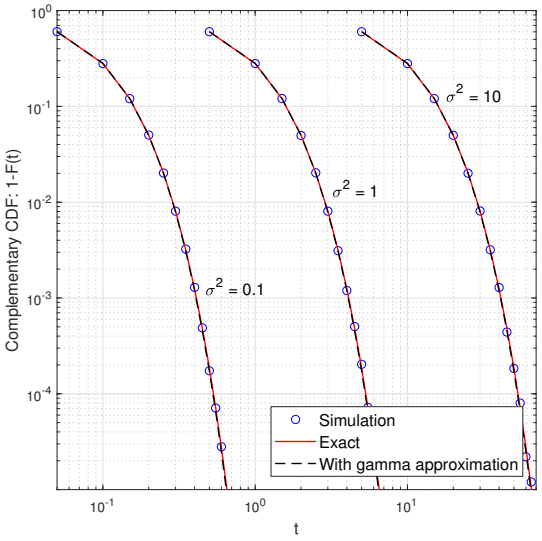

Fig. 2: The complementary CDF (CCDF) of ζ_ℓ.

With numerical calculation, we get $\mathcal{D}_{\text{KL}} \approx 0.00023$ for $\sigma^2 \in (0, 1000]$ where this very small value confirms the accuracy of the above formulation. Moreover, Fig. 2 plots the complementary cumulative distribution function (CCDF) of ζ_ℓ based on the simulation, the exact CDF in (7) and the approximate CDF in (8) which confirms the validity of the approximation. The accuracy of the approximation is also shown by the performance curves in Section IV.

Recalling that the instantaneous SINR is $\gamma = \rho\left(\sum_{\ell=1}^{L}\zeta_\ell\right)^2$. Armed with the above lemma and the fact that the rv ζ is then a sum of L i.i.d. Gamma rvs with the parameters k and θ, the rv ζ also follows a Gamma distribution with Lk and θ parameters. Therefore, the outage probability can be written as

$$P_{\text{out}|\text{L}\ge 2}(\gamma_{\text{th}}) \approx \frac{1}{\Gamma(Lk)}\gamma\left(Lk, \frac{1}{\theta}\sqrt{\frac{\gamma_{\text{th}}}{\rho}}\right) \tag{9}$$

C. Throughput

The throughput is expressed as $\log_2(1+\mathsf{SINR})$ [bits/sec/Hz]. Then, the average throughput can be evaluated as $\mathsf{R} = \int_0^{\infty}\log_2(1+x)\,f_\gamma(x)\,\mathrm{d}x$ where $f_\gamma(x)$ is the probability density function (PDF) of γ. By employing integration by parts, R can be evaluated as

$$\mathsf{R} = \frac{1}{\log(2)}\int_0^{\infty}\frac{1-F_\gamma(x)}{1+x}\,\mathrm{d}x \text{ [bits/sec/Hz]}. \tag{10}$$

1) When $L = 1$: With the aid of (6) and (10), the average throughput can be evaluated as

$$\begin{aligned} \mathsf{R}_{\text{L}=1}(\rho) &= \frac{1}{\log(2)}\frac{2}{\sigma^2\sqrt{\rho}}\int_0^{\infty}\frac{\sqrt{x}}{(1+x)}\mathsf{K}_1\left(\frac{2}{\sigma^2}\sqrt{\frac{x}{\rho}}\right)\mathrm{d}x \\ &= \frac{1}{\log(2)\sigma^2\sqrt{\rho}}\mathsf{G}_{1,3}^{3,1}\left(\frac{1}{\sigma^4\rho}\middle|\begin{matrix}-\frac{1}{2}\\ -\frac{1}{2},-\frac{1}{2},\frac{1}{2}\end{matrix}\right) \end{aligned} \tag{11}$$

where $\mathsf{G}_{p,q}^{m,n}(\cdot)$ is the Meijer G-function [15]. Here we have represented the Bessel function in terms of Meijer G function and subsequently use [15, Eq. 7.811.5].

2) When $L \geq 2$: Thus, with the aid of (9) and (10), the average throughput can be evaluated as

$$\begin{aligned}\mathsf{R}_{\mathrm{L}\geq 2}(\rho) &\approx \frac{1}{\log(2)\Gamma(Lk)}\int_0^\infty \frac{1}{(1+x)}\Gamma\left(Lk, \frac{1}{\theta}\sqrt{\frac{x}{\rho}}\right)\mathrm{d}x \\ &= \frac{1}{\log(2)}\Bigg[2\log(\theta)+\log(\rho)+2\psi^{(0)}(Lk) \\ &\quad + \frac{{}_2\mathsf{F}_3\left(1,1;2,\frac{3}{2}-\frac{Lk}{2},2-\frac{Lk}{2};-\frac{1}{4\theta^2\rho}\right)}{\theta^2\rho\left(k^2L^2-3Lk+2\right)} \\ &\quad + \frac{\pi\rho^{-\frac{1}{2}(Lk)}}{\theta^{Lk}\Gamma(Lk)}\Bigg(\frac{{}_1\mathsf{F}_2\left(\frac{Lk}{2};\frac{1}{2},\frac{Lk}{2}+1;-\frac{1}{4\theta^2\rho}\right)}{Lk\left(\csc\left(\frac{\pi Lk}{2}\right)\right)^{-1}} \\ &\quad - \frac{{}_1\mathsf{F}_2\left(\frac{Lk}{2}+\frac{1}{2};\frac{3}{2},\frac{Lk}{2}+\frac{3}{2};-\frac{1}{4\theta^2\rho}\right)}{\sqrt{\rho}\theta(1+Lk)\left(\sec\left(\frac{\pi Lk}{2}\right)\right)^{-1}}\Bigg)\Bigg] \end{aligned} \quad (12)$$

where ${}_p\mathsf{F}_q(\cdot;\cdot;\cdot)$ is the generalized hypergeometric functions [15] and $\psi^{(0)}(z)$ is the logarithmic Gamma function [15]. Here we have represented the Gamma function in terms of hypergeometric functions and subsequently use respective integration in [15, Sec. 7.5].

D. Asymptotic Analysis

1) High SINR*:* The behavior of the outage probability at high SINR regime is given in the following theorem.

Theorem 1: For high SINR, i.e., $\rho \gg 1$, the user outage probability of L elements RIS-assisted two–way networks decreases with the rate of $(\log(\rho)/\rho)^L$ over Rayleigh fading channels.

Proof: For $L=1$, since $\mathsf{K}_1(a\sqrt{x}) \to \frac{1}{a\sqrt{x}} + \frac{\sqrt{x}}{4}a\log(x)$ for $a>0$ at $x\approx 0$ [15, eq. 8.446],

we have a high SINR approximation from (6) as

$$P_{\mathrm{out|L=1}}^{\infty}(\gamma_{\mathrm{th}}) \to \frac{\gamma_{\mathrm{th}}}{\sigma^4}\frac{\log(\rho)}{\rho} \quad (13)$$

For $L \geq 2$, we can write

$$F_{\zeta_\ell}\left(\sqrt{\frac{\gamma_{\mathrm{th}}}{\rho L^2}}\right)^L \leq \mathsf{Pr}\left(\sum_{\ell=1}^{L}\zeta_\ell \leq \sqrt{\frac{\gamma_{\mathrm{th}}}{\rho}}\right) \leq F_{\zeta_\ell}\left(\sqrt{\frac{\gamma_{\mathrm{th}}}{\rho}}\right)^L.$$

This can then be written in terms of outage probabilities as

$$\left[P_{\mathrm{out|L=1}}\left(\frac{\gamma_{\mathrm{th}}}{L^2}\right)\right]^L \leq P_{\mathrm{out|L\geq 2}}(\gamma_{\mathrm{th}}) \leq \left[P_{\mathrm{out|L=1}}(\gamma_{\mathrm{th}})\right]^L.$$

With the aid of (13), we now have

$$\left[\frac{\gamma_{\mathrm{th}}}{\sigma^4 L^2}\frac{\log(\rho)}{\rho}\right]^L \leq P_{\mathrm{out|L\geq 2}}(\gamma_{\mathrm{th}}) \leq \left[\frac{\gamma_{\mathrm{th}}}{\sigma^4}\frac{\log(\rho)}{\rho}\right]^L \quad (14)$$

which proves the theorem. ∎

However, with a traditional multiple-relay network, we observe $(1/\rho)^L$ rate. Since the end-to-end effective channel behaves as a product of two Rayleigh channels, we observe $(\log(\rho)/\rho)^L$ rate with a RIS network. This is one of the important observations found through this analysis.

The behavior of the average throughout at high SINR regime is given in the following theorem.

Theorem 2: For high SINR, i.e., $\rho \gg 1$, the user average throughput of L elements RIS-assisted two–way networks increases with the rate of $\log(\rho)$ over Rayleigh fading channels.

Proof: With the aid of asymptotic expansion of $\mathsf{G}_{p,q}^{m,n}(x|\cdots)$ at $x\approx 0$ [17], we have, for $a>0$,

$$\mathsf{G}_{1,3}^{3,1}\left(ax\,\middle|\,\begin{matrix}-\frac{1}{2}\\ -\frac{1}{2},-\frac{1}{2},\frac{1}{2}\end{matrix}\right) \to \frac{-\log(ax)-2\epsilon}{\sqrt{ax}}.$$

Then, for $L=1$, the average throughput expression in (11) can be approximated at high SINR, i.e., $\rho \gg 1$, as

$$\mathsf{R}_{\mathrm{L=1}}^{\infty} \to \frac{\log(\rho)-\log\left(\frac{1}{\sigma^4}\right)-2\epsilon}{\log(2)} \quad (15)$$

For $L \geq 2$, with the aid of (12), since the terms associated with hypergeometric functions have negligible effect at $\rho \gg 1$, the average throughput expression can be approximated as

$$\mathsf{R}_{\mathrm{L}\geq 2}^{\infty} \to \frac{\log(\rho)+2\log(\theta)+2\psi^{(0)}(Lk)}{\log(2)}. \quad (16)$$

Asymptotic expressions in (15) and (16) increase at rate $\log(\rho)$ as ρ increases, which proves the theorem. ∎

Since the residual self-interference may also be a function of the transmit power, it is worth discussing the behaviors of outage probability and average throughput when the transmit power is relatively larger than the noise and loop interference powers. For the brevity, without loss of generality, we assume $P_1 = P_2 = P$. The following lemmas provide important asymptotic results.

Lemma 2: When the transmit power is relatively larger than the noise and loop interference, i.e., $P \gg \omega, \sigma_w^2$, the outage probabilities for $L=1$ and $L\geq 2$ vary, respectively, as

$$P_{\mathrm{out|L=1}}^{\infty} \to \begin{cases} \frac{\gamma_{\mathrm{th}}(\omega+\sigma_w^2)}{\sigma^4}\frac{\log(P)}{P} & \text{for } \sigma_i^2=\omega \\ P_{\mathrm{out|L=1}}\left(\rho=\frac{1}{\omega}\right) & \text{for } \sigma_i^2=\omega P\end{cases} \quad (17)$$

and

$$P_{\mathrm{out|L\geq 2}}^{\infty} \to \begin{cases} \mathcal{G}(L,\gamma_{\mathrm{th}},\omega,\sigma)\left(\frac{\log(P)}{P}\right)^L & \text{for } \sigma_i^2=\omega \\ P_{\mathrm{out|L\geq 2}}\left(\rho=\frac{1}{\omega}\right) & \text{for } \sigma_i^2=\omega P\end{cases} \quad (18)$$

where $\mathcal{G}(L,\gamma_{\mathrm{th}},\omega,\sigma)$ is the array gain. While the outage probability decreases with the rate $\left(\frac{\log(P)}{P}\right)^L$ for $\sigma_i^2=\omega$, there is an outage floor for $\sigma_i^2=\omega P$.

Proof: In particular, we can consider two extreme cases: i) When $\sigma_i^2=\omega$, where the interference is independent of the transmit power, we have $\rho = P/(\omega+\sigma_w^2) \xrightarrow{P\gg\omega,\sigma_w^2} \rho \propto P$. Therefore, results can easily be deduced from Theorem 1; and ii) When $\sigma_i^2=\omega P$, where the interference is proportional to the transmit power, we have $\rho = P/(\omega P+\sigma_w^2) \xrightarrow{P\gg\omega,\sigma_w^2} \rho \propto 1/\omega$. This completes the proof. ∎

Lemma 3: For $P \gg \omega, \sigma_w^2$, the average throughput for $L = 1$ and $L \geq 2$ vary, respectively, as

$$\mathsf{R}_{L=1}^{\infty} \to \begin{cases} \frac{\log(P) - \log\left(\frac{\omega+\sigma_w^2}{\sigma^4}\right) - 2\epsilon}{\log(2)} & \text{for } \sigma_i^2 = \omega \\ \mathsf{R}_{L=1}\left(\rho = \frac{1}{\omega}\right) & \text{for } \sigma_i^2 = \omega P \end{cases} \quad (19)$$

and

$$\mathsf{R}_{L\geq 2}^{\infty} \to \begin{cases} \frac{\log(P) + 2\psi^{(0)}(Lk) - \log\left(\frac{\sigma_w^2+\omega}{\theta^2}\right)}{\log(2)}; & \sigma_i^2 = \omega \\ \mathsf{R}_{L\geq 2}\left(\rho = \frac{1}{\omega}\right); & \sigma_i^2 = \omega P \end{cases} . \quad (20)$$

While the average throughput increases with the rate $\log(P)$ for $\sigma_i^2 = \omega$, there is a throughput floor for $\sigma_i^2 = \omega P$.

Proof: Since the proof follows the similar steps as Lemma 2, we omit the details. ■

2) For Large L (or LIS): For a sufficiently large number L, according to the central limit theorem (CLT), the rv $\zeta = \sum_{\ell=1}^{L} \zeta_\ell$ converges to a Gaussian random variable with $\mu = L\pi\sigma^2/4$ mean and $\eta = L(16-\pi^2)\sigma^4/16$ variance. The outage probability can be evaluated for $L \gg 1$ as

$$P_{\text{out}} \approx \frac{1}{2}\left(\mathsf{erf}\left[\frac{\sqrt{\frac{\gamma_{\text{th}}}{\rho}} - \mu}{\sqrt{2\eta}}\right] + \mathsf{erf}\left[\frac{\sqrt{\frac{\gamma_{\text{th}}}{\rho}} + \mu}{\sqrt{2\eta}}\right]\right). \quad (21)$$

where $\mathsf{erf}[\cdot]$ is the Gauss error function [15].

IV. Simulation Results

We set channel variance $\sigma^2 = 1$ and the thermal noise floor -70 dBm to represent a more noisy scenario. For comparison purpose, we consider two schemes where with *Scheme 1 (one time-slot transmission)* two end-users simultaneously transmit their own data to the RIS which reflects received signal with negligible delay; with *Scheme 2 (two time-slot transmission)* the user 1 transmits its data to the user 2 in the first time slot, and vice versa in the second time slot.

A. For $L = 1$

Figures 3 and 4 show the outage probability and average throughput vs P for $L = 1$, respectively. Several observations are gained: i) Our analytical results in (6) and (11) exactly match with the simulation results, which confirms the accuracy of our analysis; ii) For different loop interference $\sigma_i^2 = \omega P^\nu$, we notice that the outage decreases at a rate of $\log(P)/P$ and the throughput increases at a rate of $\log(P)$ when $\nu = 0$, and both have floors when $\nu = 1$ due to the transmit-power dependent interference, as in (17) and (19). iii) When ω reduces from 10^{-4} to 10^{-5}, the outage and throughput improve around 9 dB and 3.32 [bits/sec/Hz], respectively, for each case; and iv) two–way communications with Scheme 2 outperforms Scheme 1 when $P < 5$ dBm and $P < 25$ dBm for $\omega = 10^{-5}$ and $\omega = 10^{-4}$, respectively, with $\nu = 0$. For $\nu = 1$, Scheme 2 outperforms Scheme 1 in the entire simulated region. Therefore, it is important to keep the effect of loop interference independent of transmit power if two–way communications use Scheme 1.

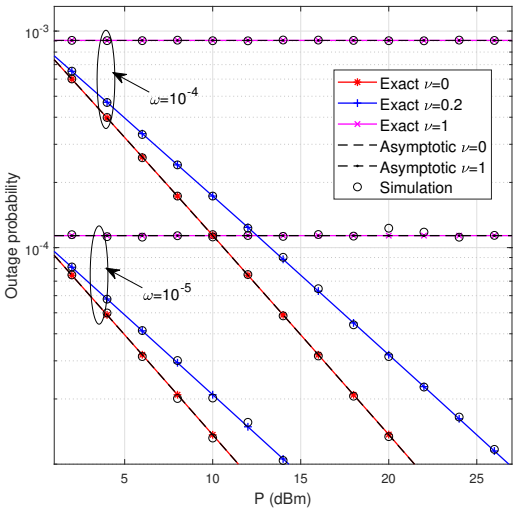

Fig. 3: The outage probability vs P when $\sigma_i^2 = 10^{-4}$.

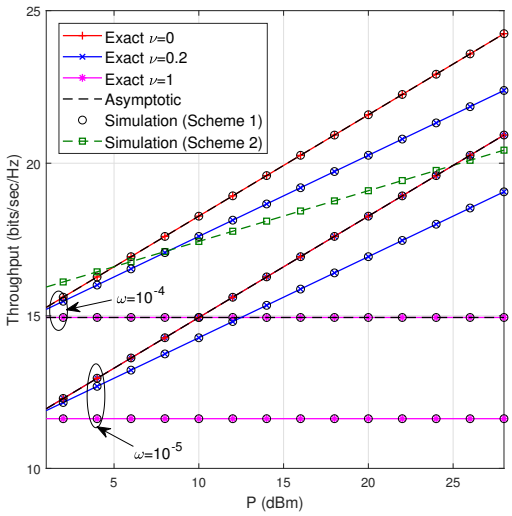

Fig. 4: The outage probability vs P when $\sigma_i^2 = 10^{-4}$.

B. For $L \geq 2$

Fig. 5 shows the outage probability vs P, when loop-interference is independent of transmit power P, i.e., $\sigma_i^2 = \omega$. For a given L, the outage probability decreases with $[\log(P)/P]^L$ which confirms Lemma 2. Although the outage probability decreases with L, the diminishing rate also decreases. For example, when we increase L from 2 to 4, we can save power around 14 dBm at 10^{-3} outage. However, for the same outage, we can only save power around 8 dBm when we increase L from 32 to 64. Interestingly, this figure confirms the accuracy of our gamma approximation. Moreover, it is more accurate than the CLT approximation even for $L = 64$.

Fig. 6 shows the average throughput vs P, when loop-interference is either independent ($\nu = 0$) or linearly-

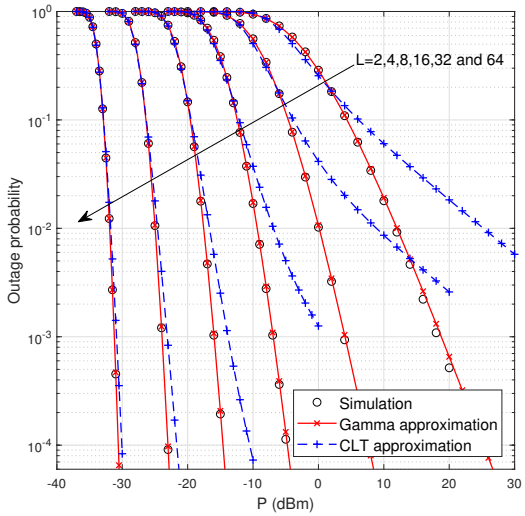

Fig. 5: The outage probability vs P when $\sigma_i^2 = 10^{-4}$.

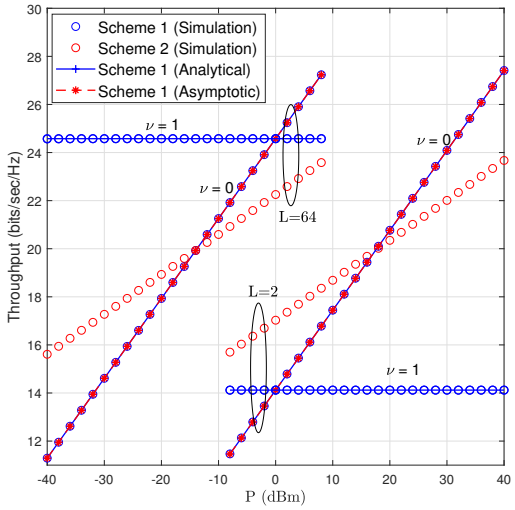

Fig. 6: The average throughput vs P with $L \geq 2$.

dependent ($\nu = 1$) of transmit power P, where $\sigma_i^2 = \omega P^{\nu}$. For any L, as shown in the figure and (20), the average throughput increases in order of $\log(P)$ when $\sigma_i^2 = \omega$, which confirms Lemma 3. Further transmit power reduces by around 19 dBm when L increases from 2 to 16. We also plot the throughput of Scheme 1 and Scheme 2 where Scheme 1 starts to outperform Scheme 2 when P increases where transition happens at $P \approx 17.5, -14.0$ dBm for $L = 2, 64$, respectively. For $\sigma_i^2 = \omega P$ ($\nu = 1$), we have throughput floors because loop-interference enhances with transmit power in Scheme 1. Due to this reason, as shown in the figure, Scheme 2 outperforms Scheme 1 when P increases.

V. Conclusion

RIS assisted systems have been proposed for two–way wireless communications. For the optimal phases of the RIS elements over reciprocal channels, the exact outage probability and throughput have been derived for a single-element RIS. Since the exact performance analysis for a multiple-element RIS seems intractable, approximations are derived for outage probability and average throughput. In this respect, a product of two Rayleigh random variables is approximated by a gamma random variable. Moreover, asymptotic analysis has been conducted for high SINR ρ regime. Our analysis reveals that the outage probability decreases at the rate of $(\log(\rho)/\rho)^L$, whereas throughput increases at the rate of $\log(\rho)$. We could observe either an outage or throughput floor caused by transmit power dependent loop interference. Simulation results illustrate that the rate of throughput increment or transmit power saving reduces when number of elements increases.

References

[1] M. D. Renzo *et al.*, "Smart radio environments empowered by reconfigurable AI meta-surfaces: an idea whose time has come," *EURASIP J. Wireless Commun. Netw.*, vol. 2019, no. 1, p. 129, Dec. 2019.

[2] S. Atapattu, P. Dharmawansa, C. Tellambura, and J. Evans, "Exact outage analysis of multiple-user downlink with MIMO matched-filter precoding," *IEEE Commun. Lett.*, vol. 21, no. 12, pp. 2754–2757, Dec. 2017.

[3] T. L. Marzetta, "Noncooperative cellular wireless with unlimited numbers of base station antennas," *IEEE Trans. Wireless Commun.*, vol. 9, no. 11, pp. 3590–3600, Nov. 2010.

[4] S. Atapattu, Y. Jing, H. Jiang, and C. Tellambura, "Relay selection and performance analysis in multiple-user networks," *IEEE J. Select. Areas Commun.*, vol. 31, no. 8, pp. 1517–1529, Aug. 2013.

[5] C. Huang, A. Zappone, G. C. Alexandropoulos, M. Debbah, and C. Yuen, "Reconfigurable intelligent surfaces for energy efficiency in wireless communication," *IEEE Trans. Wireless Commun.*, vol. 18, no. 8, pp. 4157–4170, Aug. 2019.

[6] Q. Wu and R. Zhang, "Intelligent reflecting surface enhanced wireless network: Joint active and passive beamforming design," in *IEEE Global Telecommn. Conf. (GLOBECOM)*, Dec. 2018.

[7] M. Cui, G. Zhang, and R. Zhang, "Secure wireless communication via intelligent reflecting surface," *IEEE Wireless Commun. Lett.*, 2019.

[8] H. Shen, W. Xu, W. Xu, S. Gong, Z. He, and C. Zhao, "Secrecy rate maximization for intelligent reflecting surface assisted multi-antenna communications," *IEEE Commun. Lett.*, 2019.

[9] Y. Han, W. Tang, S. Jin, C. Wen, and X. Ma, "Large intelligent surface-assisted wireless communication exploiting statistical CSI," *IEEE Trans. Veh. Technol.*, vol. 68, no. 8, pp. 8238–8242, Aug. 2019.

[10] M. Jung, W. Saad, Y. Jang, G. Kong, and S. Choi, "Performance analysis of large intelligent surfaces (LISs): Asymptotic data rate and channel hardening effects," *IEEE Trans. Wireless Commun.*, 2020.

[11] E. Basar, M. Di Renzo, J. De Rosny, M. Debbah, M. Alouini, and R. Zhang, "Wireless communications through reconfigurable intelligent surfaces," *IEEE Access*, vol. 7, pp. 116 753–116 773, 2019.

[12] M. Badiu and J. P. Coon, "Communication through a large reflecting surface with phase errors," *IEEE Wireless Commun. Lett.*, pp. 1–1, 2019.

[13] S. Atapattu, Y. Jing, H. Jiang, and C. Tellambura, "Relay selection schemes and performance analysis approximations for two-way networks," *IEEE Trans. Commun.*, vol. 61, no. 3, pp. 987–998, Mar. 2013.

[14] S. Atapattu, P. Dharmawansa, M. Di Renzo, C. Tellambura, and J. S. Evans, "Multi-user relay selection for full-duplex radio," *IEEE Trans. Commun.*, vol. 67, no. 2, pp. 955–972, Feb. 2019.

[15] I. S. Gradshteyn and I. M. Ryzhik, *Table of Integrals, Series and Products*, 7th ed. Academic Press Inc, 2007.

[16] S. Atapattu, C. Tellambura, and H. Jiang, "A mixture gamma distribution to model the SNR of wireless channels," *IEEE Trans. Wireless Commun.*, vol. 10, no. 12, pp. 4193–4203, Dec. 2011.

[17] "Mathematica, Version 12.0," http://functions.wolfram.com/ HypergeometricFunctions/MeijerG/06/01/03/01/0003/, accessed: 2019-12-30.